High resolution projections of cropping season atmospheric evaporative demand in the African Sahel

Laura Harrison
Department of Geography, University of California, Santa Barbara
harrison@geog.ucsb.edu

Laura Harrison[1]; Joel Michaelsen[1]; Chris Funk[1,2]; Elena Tarnavsky[3]; Michael Marshall[2]; Molly Brown[4]
[1]UC Santa Barbara, USA [2] USGS [3] University of Reading, UK [4] NASA Goddard Space Flight Center

Background

Atmospheric evaporative demand (potential evapotranspiration, PET) is a measure of the atmospheric component of the hydrologic system. It is routinely used for monitoring vegetative stress and water resources. With other atmospheric features unchanged higher temperature increases PET (Clausius-Clapeyron relation) and plant water requirements. When surface moisture is not able to constrain sensible heating, positive temperature feedbacks [1] and increased risk of agricultural drought may result.

The goal is to identify how growing season PET may change in the Sahel over the next several decades. Projected warming and limited adaptive capacity in the Sahel necessitate medium-term outlooks with high enough confidence and spatial-temporal detail for food security planning. Strong relationships between observed PET and temperature anomalies identify areas of high predictability.

Strategy

We build a predictive statistical model with PET and temperature observations. Daily average temperature anomalies are used to predict PET anomalies during the June-September rainy season (2001-2010). This presentation shares results on this topic. Where this model explains observed daily PET variations we will use it to estimate PET changes to 2050 given IPCC AR4 temperature projections.

This strategy side-steps uncertainties of the common method of PET projections [2], in which PET changes are estimated with climate variables *all* from GCM projections. Aside from temperature projections GCM output is highly uncertain in the Sahel. GCM ability to recreate West African annual rainfall is shown in Figure 1.

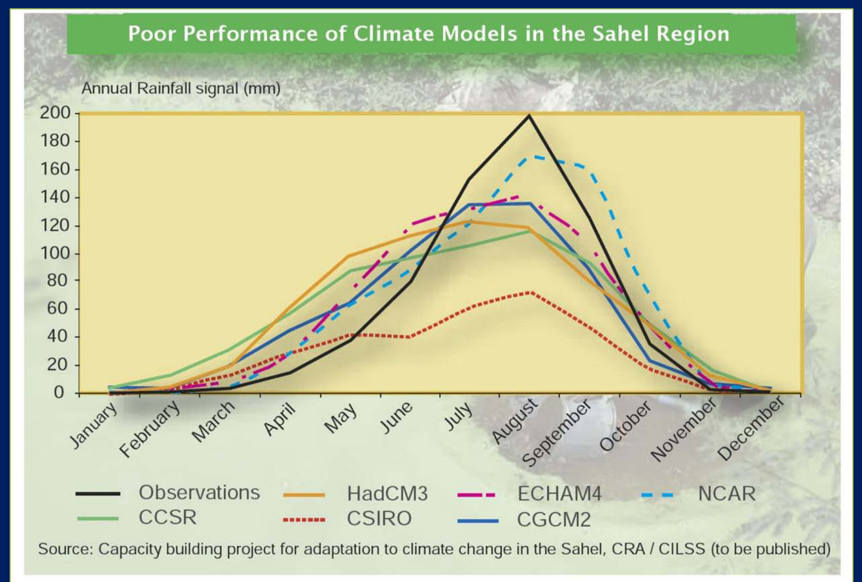

Figure 1. Annual Sahel rainfall: Observations and GCM simulation. Source: Atlas on Regional Integration in West Africa ECOWAS-SWAC/OECD©2008 – January 2008

Climate data and PET estimates

Noah 2.7.1 Land Surface Model output from the Global Land Data Assimilation System (GLDAS). Data is 3-hourly at 0.25 degree spatial resolution. Daily average temperature and daytime total PET are computed for June-September 2001-10. Anomalies are the deviation from daily means estimated by quadratic seasonal curves.

PET is calculated with the physically-based FAO-56 Penman-Monteith equation [3] for reference evapotranspiration (ET_o). ET_o is an ideal form to work with because values refer to the PET from the same reference surface and can be directly compared across space/time. PM-FAO56 is the international standard for ET_o [4].

$$ET_o = \frac{\Delta(R_n - G)}{\lambda[\Delta + \gamma(1 + C_d u_2)]} + \frac{\gamma \frac{37}{T_a + 273.16} u_2 (e_s - e_a)}{\Delta + \gamma(1 + C_d u_2)}$$

Where

ET_o = grass reference evapotranspiration (mm h^{-1})
Δ = slope of saturation vapor pressure curve (kPa °C^{-1}) at T_a
R_n = net radiation (MJ $m^{-2}h^{-1}$)
G = soil heat flux density (MJ $m^{-2}h^{-1}$)
γ = psychrometric constant (kPa °C^{-1})
T_a = mean hourly air temperature
u_2 = wind speed at 2 meters (m s^{-1})
e_s = saturation vapor pressure (kPa) at T_a
e_a = actual vapor pressure (kPa) at T_a
λ = latent heat of vaporization (MJ $m^{-2}h^{-1}$)
C_d = bulk surface resistance and aerodynamic resistance coefficient

Equation 1. FAO56-PM hourly reference evapotranspiration equation for a grass reference surface. 3-hourly estimates during R_n>0 are calculated and summed to daily daytime total ET_o (mm day^{-1}). Soil heat flux (G) is calculated as 0.1*R_n. Surface and aerodynamic resistance is 0.24 [5].

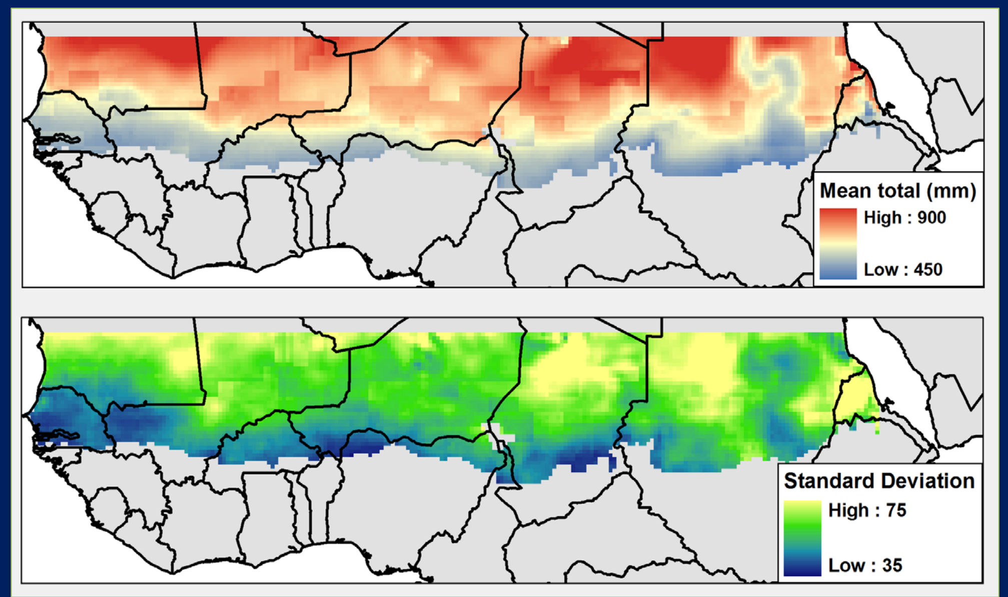

Figure 2. June-September Sahel PET.

Study area

Analysis is focused within the Sahel (10N-20N, 20W -40E) to areas where similar climate mechanisms influence PET. Exploratory analysis indicates the advection component (2nd term in PM-FAO56) is an important driver of PET fluctuations. The study area is subset to where the advection component variance is at least 40% of the radiation component (1st term) variance. June-September total PET (mm) and interannual standard deviation are shown in Figure 2.

Predictive model

To measure the influence of temperature on PET anomalies at each location we use an ARIMA(1,0,0) model. This form of regression model corrects for autocorrelated errors anticipated from exploratory analysis. PET anomalies through the growing season exhibit moderate autocorrelation (~1 day lag), likely due to persistence of weather events.

$$y(t) = \alpha * y(t-1) + \beta * x(t) + \gamma + \varepsilon$$

Where
- $y(t)$ is daily PET anomaly (mm)
- α is PET autocorrelation coefficient for lag 1
- β is slope coefficient for temperature anomaly (mm °C^{-1} day^{-1})
- γ is intercept term
- ε is model error

The model has two predictive components: A first order autocorrelation component and a linear regression component (temperature). Parameters are estimated with maximum likelihood method. Separate models are fit to each month to capture intra seasonal variability.

Results

Mapped autocorrelation coefficients for June-September (Figure 3) show a west to east (and south to north) gradient in autocorrelation strength. This spatial pattern indicates influence of the tropical Atlantic Ocean on regional weather patterns. Highly variable convective storms are the dominant source of summer rainfall in the south and west.

The PET autocorrelation component is statistically significant across much of the region through the growing season with exception of southern areas during the crux of seasonal rains (July and August). Most locations exhibit strongest autocorrelation in September. Persistence of PET anomalies are consistently strong (0.4-0.7) in dry areas of northern Niger, Chad, and Sudan.

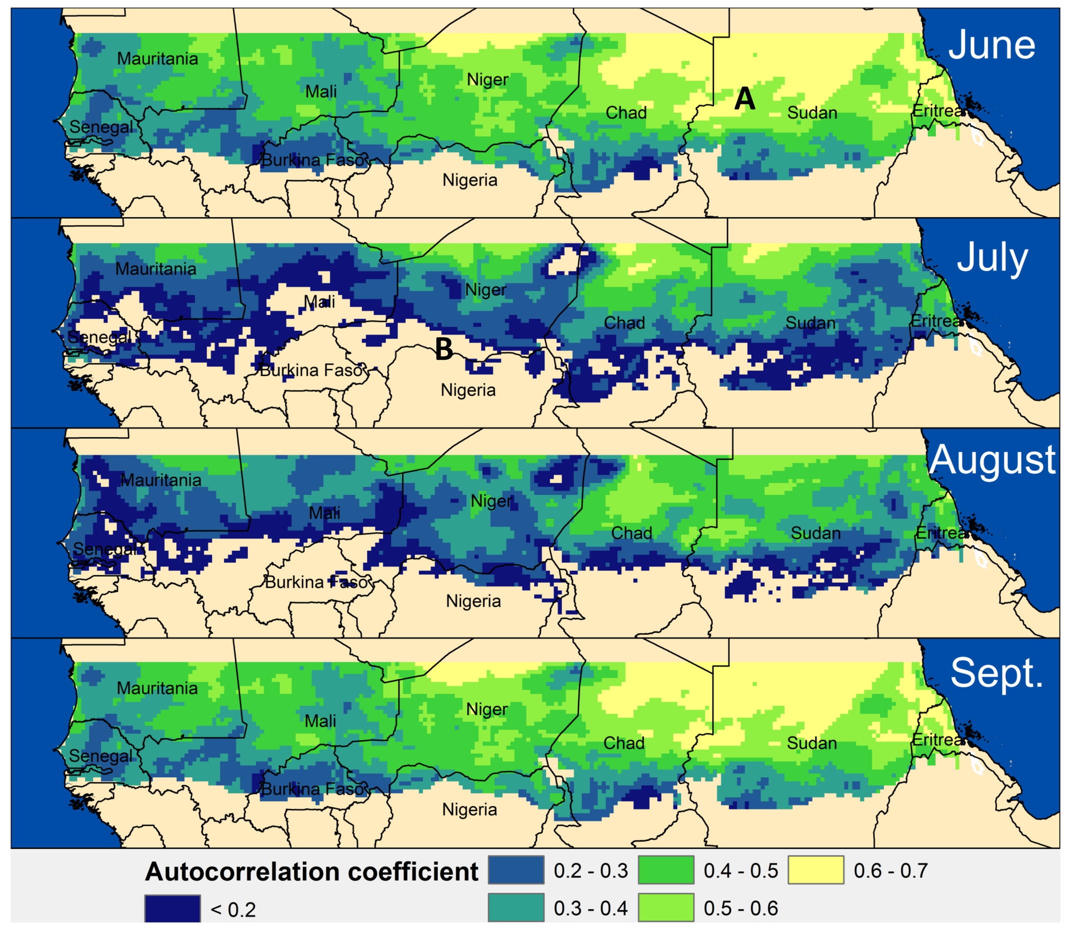

Figure 3. Autocorrelation coefficient for June-September, masked for statistical significance by t-value < 1.96.

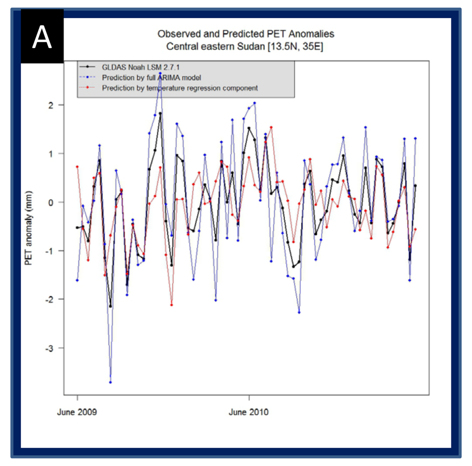

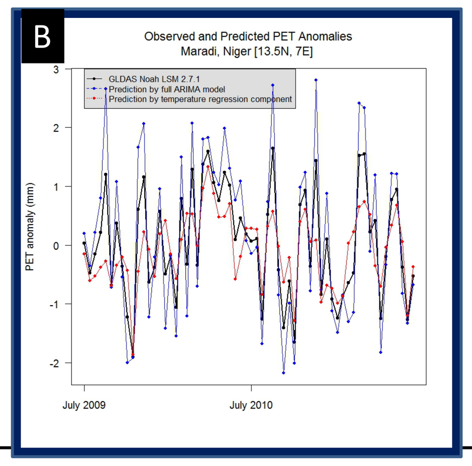

Time series of observed and modeled PET anomalies at selected locations for June (Box A) and July (Box B) show the full ARIMA model and the temperature regression component of this model both capture daily observed variation. Temperature alone sufficiently predicts the direction and relative intensity of PET anomalies. The autocorrelation component improves model explanation of temporal pattern.

Mapped temperature slope coefficients (Figure 4) show a statistically significant moderate-to-strong relationship between temperature and PET anomalies across most of the region. The period of greatest strength (July-September) aligns with regional occupation of the West African summer monsoon. Intense summer insolation and monsoon-driven variations in cloud cover establish a physical link between temperature and net radiation, leading to positive PET anomalies during hot and dry monsoon phases. Of particular interest for Sahelian agriculture are pockets of 0.4-0.5 mm °C^{-1} day^{-1} coefficient values (green) in the southern region of the study area in August, the period of highest crop sensitivity to heat and moisture stress. 1°C of warming is associated with a 12-16 mm loss of surface moisture (August total).

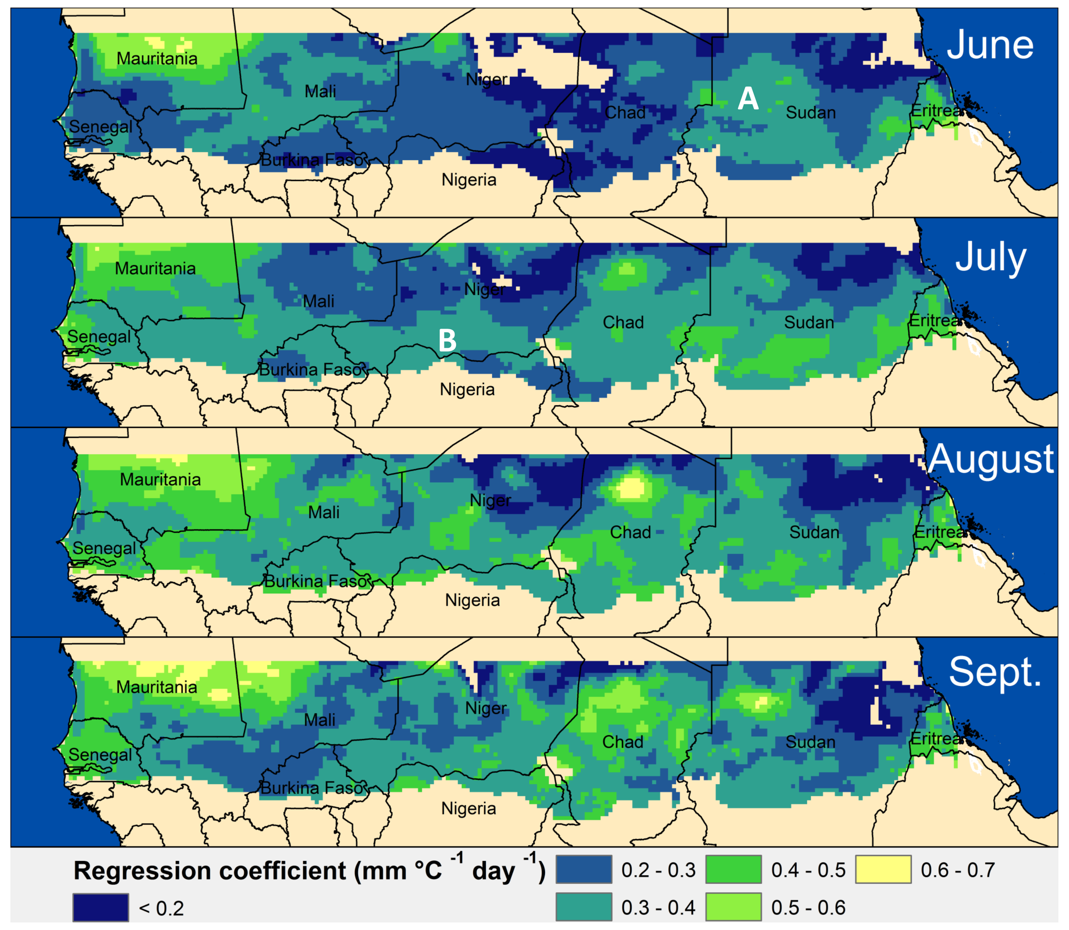

Figure 4. Temperature regression coefficient for June-September, masked for statistical significance by t-value < 1.96.

Large PET anomalies are difficult to model, as shown by consistent under prediction by the temperature regression and over prediction with the full ARIMA model. Spatial and temporal variation in model performance indicates influence of other meteorological variables, of which humidity and wind are suspected as important. However, low confidence in climate model projections of these variables in the Sahel make them undesirable as additional predictor variables.

Mapped R^2 values for June, August, and September (Figure 5) show the predictive model best explains variance of PET anomalies in the southern (agricultural) region of the Sahel (R^2 0.4-0.6). Model fit is generally highest during mid season (July-August). In southern Sudan and Eritrea > 60% of PET anomaly variance early in the growing season is described by the model.

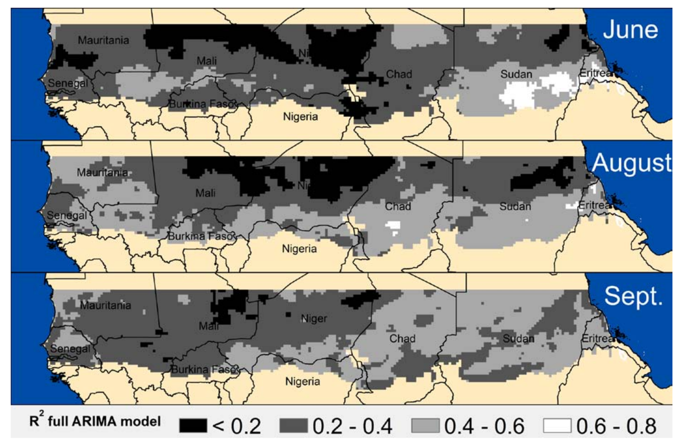

Figure 5. Mapped R^2 values of full ARIMA model for beginning, middle, and end of growing season (June, August, and September).

Most of the variance explained by the model is due to the temperature component, as shown by the ratio of the linear regression component R^2 to the full ARIMA model R^2 (below).

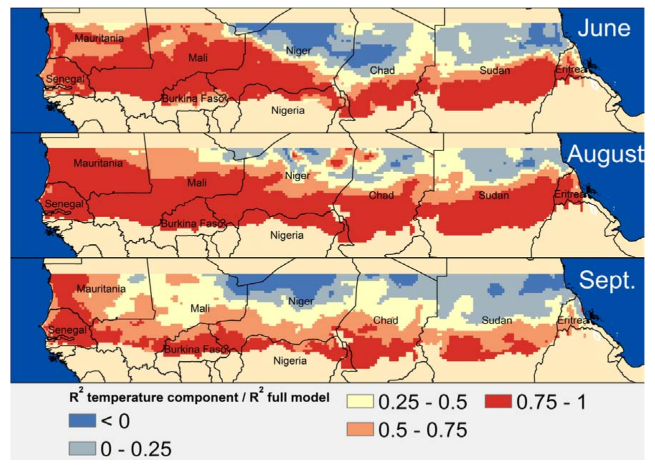

For vast expanses of the western and southern Sahel during the middle of the growing season temperature is responsible for 75-100% of the model's explanatory power. In the dry northeast temperature alone is a poor predictor of PET anomalies.

Conclusions

In theory warming increases PET by enhancing the water holding capacity of the atmosphere. In reality other atmospheric conditions are also important. We have shown strong potential in the Sahel for recent historical PET estimates (that consider all relevant meteorological variables) to be extended for PET projections through the next several decades.

We have identified a straightforward predictive model for PET anomalies using temperature as the only independent predictor. This method is ideal because it does not incorporate large uncertainties of climate models and can identify "hot spots" of projected PET change.

Agricultural areas in the southern Sahel during the crux of the growing season exhibit highest predictability. "Hot spots" within this region/period are found in areas of Mauritania, Senegal, Mali, Burkina Faso, Niger, Nigeria, Chad, Sudan, and Eritrea.

Further work will explore model residuals to examine the role of humidity and to identify a treatment for over prediction of large anomalies by the autocorrelation component.

References

1. Priestley, C.H.B.(1966). The limitation of temperature by evaporation in hot climates, Agricultural Meteorology, Volume 3, Issues 3-4, May 1966, Pages 241-246, ISSN 0002-1571, 10.1016/0002-1571(66)90031-8.
2. Kingston, D. G., M. C. Todd, R. G. Taylor, J. R. Thompson, and N. W. Arnell (2009). Uncertainty in the estimation of potential evapotranspiration under climate change, *Geophys. Res. Lett.*, 36, L20403, doi:10.1029/2009GL040267.
3. Allen, R. G., L. S. Pereira, D. Raes, and M. Smith (1998), Crop Evapotranspiration: Guidelines for Computing Crop Water Requirements, Irrig. Drain. Pap. 56, Food and Agric. Org., U. N., Rome.
4. International Commission for Irrigation and Drainage (ICID) and the Food and Agriculture Organization of the United Nations (FAO) Expert Consultation on Revision of FAO Methodologies for Crop Water Requirements
5. ASCE Task Committee on Standardization of Reference Evapotranspiration (2000)